Simulation of positive operator-valued measures and quantum instruments via quantum state-preparation algorithms

Douglas F. Pinto [1,*] Marcelo S. Zanetti [2,†] Marcos L. W. Basso [3,‡] and Jonas Maziero [1,§]

[1] *Physics Department, Center for Natural and Exact Sciences, Federal University of Santa Maria, Roraima Avenue 1000, Santa Maria, Rio Grande do Sul, 97105-900, Brazil*

[2] *Department of Electronics and Computing, Technology Center, Federal University of Santa Maria, Roraima Avenue 1000, Santa Maria, Rio Grande do Sul, 97105-900, Brazil*

[3] *Center for Natural and Human Sciences, Federal University of the ABC, States Avenue 5001, Santo André, São Paulo, 09210-580, Brazil*

(Received 29 November 2022; accepted 25 January 2023; published 9 February 2023)

In Phys. Rev. A **100**, 062317 (2019), the authors reported an algorithm to implement, in a circuit-based quantum computer, a general quantum measurement (GQM) of a two-level quantum system, a qubit. Even though their algorithm seems right, its application involves the solution of an intricate nonlinear system of equations to obtain the angles determining the quantum circuit to be implemented for the simulation. In this article, we identify and discuss a simple way to circumvent this issue and implement GQMs on any d-level quantum system through quantum state preparation algorithms. Using some examples for one qubit, one qutrit, and two qubits, we illustrate the easy of application of our protocol. In addition, we show how one can utilize our protocol for simulating quantum instruments, for which we also give an example. All our examples are demonstrated using IBM's quantum processors.

DOI: 10.1103/PhysRevA.107.022411

I. INTRODUCTION

One of the basic postulates of quantum mechanics says that the measurement of an observable, represented by a Hermitian operator $A = \sum_{j=1}^{d_A} a_j \Pi_j^A$, is described by the projection operators Π_j^A, i.e., $\Pi_j^A \Pi_k^A = \delta_{jk} \Pi_j^A$ and $\sum_{j=1}^{d_A} \Pi_j^A = \mathbb{I}_A$, with d_A being the dimension of the system Hilbert space $\mathcal{H}_A$ and $\mathbb{I}_A$ is the identity operator on $\mathcal{H}_A$. For a quantum system A prepared in the state ρ_A, the measurement outcome corresponding to Π_j^A is obtained with probability $\Pr(\Pi_j^A|\rho_A) = \mathrm{Tr}(\Pi_j^A \rho_A \Pi_j^A)$ and the postmeasurement state is $\Pi_j^A \rho_A \Pi_j^A / \mathrm{Tr}(\Pi_j^A \rho_A \Pi_j^A)$. Eventually, researchers realized that more general quantum measurements (GQMs) can be defined. These measurements, also named positive operator-value measurements (POVMs), are described by a set of measurement operators $\{M_j\}$ in $\mathcal{H}_A$ that satisfy the completeness relation $\sum_j M_j^\dagger M_j = \mathbb{I}_A$. In this general setting, for a system prepared in the state ρ_A, the probability of obtaining the measurement result corresponding to M_j is $\Pr(M_j|\rho_A) = \mathrm{Tr}(M_j \rho_A M_j^\dagger)$ and the postmeasurement state is $M_j \rho_A M_j^\dagger / \mathrm{Tr}(M_j \rho_A M_j^\dagger)$. The fact that $\Pr(M_j|\rho_A) = \mathrm{Tr}(E_j \rho_A) \geqslant 0$ with $E_j = M_j^\dagger M_j$ being positive-semi-definite operators motivates the name POVM. The completeness restriction ensures that $\sum_j \Pr(M_j|\rho_A) = 1$ [1,2].

POVMs provide advantages in several applications in quantum information science (QIS), as, for example, in quantum state estimation [3], shadow quantum state tomography [4], discrimination of quantum states [5], randomness certification [6], acquisition of information from a quantum source [7], quantum key distribution [8], Bell inequalities [9], and device-independent quantum information protocols [10]. So, experimentally implementing POVMs is of fundamental importance for QIS and considerable work has been done in this direction recently, as, for example, in Refs. [11–20].

Of particular interest to us here is Ref. [20], where the authors proposed a deterministic protocol to implement single-qubit POVMs on quantum computers. Even though their protocol seems correct, we realize that for applying it one first has to solve complicated nonlinear systems of equations for obtaining the angles determining the quantum circuit to be used in the simulation. Then, motivated by their work, here we identify and discuss a simple way to implement POVMs on any d_A-level quantum system through quantum state preparation (QSP) algorithms [21–28]. Using some examples for $d_A = 2$, $d_A = 3$, and $d_A = 4$ we illustrate the simplicity and convenience for application of this new method. In addition to that, we apply our protocol for the simulation of quantum instruments [2].

A POVM with elements $\{M_j\}$ can be implemented coherently through an isometric transformation [2]

$$V_{AB}|k\rangle_A \otimes |0\rangle_B := \sum_j (M_j|k\rangle_A) \otimes |j-1\rangle_B, \tag{1}$$

followed by a selective projective measurement in the basis $\{|j\rangle_B\}$ of the auxiliary system B, plus discarding of the system B. Above $|j\rangle_S$ is the computational basis for the system $S = A, B$. This procedure produces the same statistics and postmeasurement states of the system A as does the

*douglasfpinto@gmail.com
†marcelo.zanetti@ufsm.br
‡marcoslwbasso@hotmail.com
§jonas.maziero@ufsm.br

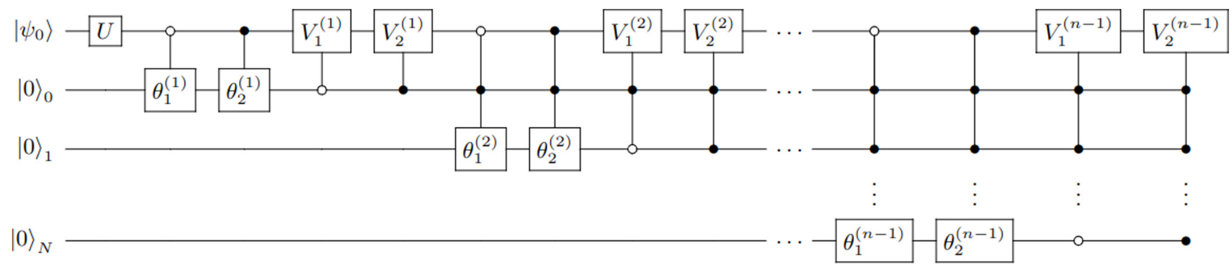

FIG. 1. Adapted from the quantum circuit reported in Ref. [20] to simulate general one-qubit POVMs. U and $V_j^{(k)}$ are general one-qubit gates and $\theta_j^{(k)}$ represents the $R_y(\theta_j^{(k)})$ gate. We also used $N = \log_2 n$.

POVM $\{M_j\}$, that is to say, $\Pr(|j\rangle_B|\tilde{\rho}_{AB}) = \Pr(M_j|\rho_A)$ with $\tilde{\rho}_{AB} = V_{AB}(\rho_A \otimes |0\rangle_B\langle 0|)V_{AB}^\dagger$ and $\mathrm{Tr}_B(\mathbb{I}_A \otimes |j\rangle_B \langle j|)\tilde{\rho}_{AB}(\mathbb{I}_A \otimes |j\rangle_B\langle j|)/\mathrm{Tr}[(\mathbb{I}_A \otimes |j\rangle_B\langle j|]\tilde{\rho}_{AB}(\mathbb{I}_A \otimes |j\rangle_B\langle j|)) = M_j\rho_A M_j^\dagger/\mathrm{Tr}(M_j\rho_A M_j^\dagger)$, with ρ_A being the premeasurement state of system A. So attempts to implement POVMs experimentally usually start from Eq. (1).

The protocol given in Ref. [20] follows this path. The authors said that the quantum circuit shown in Fig. 1 prepares the state

$$|\Psi\rangle = \sum_{j=1}^{n-1}(M_j|\psi_0\rangle) \otimes |o_1^{(j)}\rangle + (M_n|\psi_0\rangle) \otimes |o_2^{(n-1)}\rangle, \quad (2)$$

with $|\psi_0\rangle$ being the system A premeasurement state and $\{|o_1^{(j)}\rangle\}, |o_2^{(n-1)}\rangle\}$ are orthonormal states of the auxiliary system B, thus implementing a one-qubit POVM with an arbitrary number n of elements

$$M_j = \begin{cases} V_1^{(1)}D_1^{(1)}U, \text{ para } j = 1, \\ V_1^{(j)}D_1^{(j)}\Pi_{k=1}^{j-1}V_2^{(k)}D_2^{(k)}U, \text{ para } 1 < j < n, \\ \Pi_{k=1}^{n-1}V_2^{(k)}D_2^{(k)}U, \text{ para } j = n. \end{cases} \quad (3)$$

In theses equations, U and $V_j^{(k)}$ are general one-qubit unitaries and $D_1^{(k)} = \cos\theta_1^{(k)}|0\rangle\langle 0| + \cos\theta_2^{(k)}|1\rangle\langle 1|$ and $D_2^{(k)} = \sin\theta_1^{(k)}|0\rangle\langle 0| + \sin\theta_2^{(k)}|1\rangle\langle 1|$ are positive operators if $\theta_1^{(k)}, \theta_2^{(k)} \in [0, \pi/2]$.

As a general one-qubit unitary transformation can be recast in terms of four angles as [1] $\begin{bmatrix} e^{i(\alpha-\beta/2-\delta/2)}\cos\frac{\gamma}{2} & -e^{i(\alpha-\beta/2+\delta/2)}\sin\frac{\gamma}{2} \\ e^{i(\alpha+\beta/2-\delta/2)}\sin\frac{\gamma}{2} & e^{i(\alpha+\beta/2+\delta/2)}\cos\frac{\gamma}{2} \end{bmatrix}$, we see that, given the matrices for the POVM elements in the left-hand side of Eq. (3), the implementation of the algorithm of Ref. [20] involves the solution of an intricate system of nonlinear equations for the angles appearing on the right-hand side of Eq. (3). Perhaps this complication is related to the wrong examples presented in Ref. [20], for which the measurement operators do not satisfy the completeness restriction. It is worthwhile mentioning also that the protocol of Ref. [20], if implemented exactly as in the quantum circuit of Fig. 1, requires $\mathcal{O}(n)$ auxiliary qubits. For diminishing this number to $\mathcal{O}(\log_2 n)$, one has to make some modifications or additions to this quantum circuit, as exemplified in Fig. 2 for $n = 4$.

II. PROTOCOL AND APPLICATION EXAMPLES

Quantum state preparation (QSP) algorithms are used as subroutines for performing many tasks [21–28], as, for example, for implementing the general quantum Fourier transform [21]. Motivated by the issues just discussed about the POVM simulation algorithm of Ref. [20], here we present a simple protocol that implements POVMs on any discrete quantum system A associated with a Hilbert space $\mathcal{H}_A$ through QSP algorithms. For the dimension d_A of the system A on which the POVM is to be implemented and any number of elements of the POVM, if the measurement operators M_j are known, in principle it is possible to calculate the right-hand side of Eq. (1):

$$|\Psi\rangle_{AB} = \sum_j \left(M_j|k\rangle_A\right) \otimes |j-1\rangle_B. \quad (4)$$

Once obtained this vector, we can use QSP algorithms to prepare it. Afterwards, a projective measurement on the basis $\{|j\rangle_B\}$ is done. Running several times this procedure, we can extract the probabilities. It is worthwhile to mention that, since the projective measurements are done on the system B, by applying postselection we can use quantum state tomography to obtain the postmeasurement state of the system A. Therefore, our protocol can be summarized as follows.

(1) Given $\{M_j\}$, obtain $|\Psi\rangle_{AB}$ of Eq. (4).

(2) Implement $|\Psi\rangle_{AB}$ using algorithms for quantum state preparation.

(3) Make projective measurements on system B and extract the measurement statistics.

(4) If needed, implement quantum state tomography to obtain the system A postmeasurement state, with postselection of the measurement results on system B.

This protocol works for any dimension of the system A. The minimum dimension of the auxiliary system B is equal to the number of POVM elements, independently of the dimension of the system A, i.e., our protocol uses $\mathcal{O}(\log_2 n)$ auxiliary qubits. Of course, for implementing our protocol on quantum computers based on qubits, it is necessary to choose how to codify the qudit states in terms of qubit states.

In the sequence we present examples of applications of our protocol. Let us start by considering a one-qubit POVM with two elements:

$$M_1 = \frac{1}{2\sqrt{2}}(|0\rangle\langle 0| + \sqrt{3}|1\rangle\langle 0| + 2|1\rangle\langle 1|), \quad (5)$$

$$M_2 = \frac{1}{2\sqrt{2}}(|0\rangle\langle 0| - \sqrt{3}|1\rangle\langle 0| + 2|1\rangle\langle 1|). \quad (6)$$

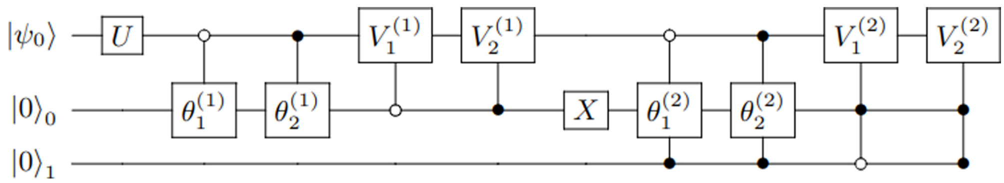

FIG. 2. Adaptation of the quantum circuit of Ref. [20], shown in Fig. 1, for simulating a four-elements one-qubit POVM.

We set the premeasurement state of system A to $|0\rangle_A$. So the POVM probabilities are given by

$$Pr(M_1|0) = \langle 0|M_1^\dagger M_1|0\rangle = 1/2, \tag{7}$$

$$Pr(M_2|0) = \langle 0|M_2^\dagger M_2|0\rangle = 1/2. \tag{8}$$

In this case we use a qubit as the auxiliary system B. For implementing our protocol, we have to prepare the state

$$|\Psi_{AB}\rangle = 2^{-3/2}(|00\rangle + \sqrt{3}|10\rangle + |01\rangle - \sqrt{3}|11\rangle). \tag{9}$$

Here we use the algorithm of Ref. [22] for QSP. This algorithm was already implemented in QISKIT [30]. After state preparation, a projective measurement is performed in the basis $\{|0\rangle_B, |1\rangle_B\}$. For performing the demonstrations, we used the IBMQ [29] quantum chip *ibmq_belem*. The simulation and demonstration results for this first example are shown in Fig. 3. Some relevant calibration parameters of the quantum chips used for the demonstrations reported in this article are presented in the Appendix.

As a second example, let us consider a one-qubit three-element POVM with measurement elements associated with the sequence of states in the xz plane of the Bloch sphere separated by $2\pi/3$ radians

$$M_1 = \sqrt{\frac{2}{3}}|0\rangle\langle 0|, \tag{10}$$

$$M_2 = \sqrt{\frac{2}{3}}|\psi(2\pi/3, 0)\rangle\langle\psi(2\pi/3, 0)|, \tag{11}$$

$$M_3 = \sqrt{\frac{2}{3}}|\psi(4\pi/3, 0)\rangle\langle\psi(4\pi/3, 0)|, \tag{12}$$

with $|\psi(\theta,\phi)\rangle = \cos(\frac{\theta}{2})|0\rangle + \sin(\frac{\theta}{2})e^{i\phi}|1\rangle$. The implementation of this POVM follows the same recipe as for the previous example. In this case the global state to be prepared is

$$\begin{aligned}|\Psi_{Abc}\rangle = \frac{1}{4}\sqrt{\frac{2}{3}}(|0\rangle_A \otimes |01\rangle_{bc} + |0\rangle_A \otimes |10\rangle_{bc}) \\ + \sqrt{\frac{2}{3}}|0\rangle_A \otimes |00\rangle_{bc} \\ + \frac{\sqrt{2}}{4}(|1\rangle_A \otimes |01\rangle_{bc} - |1\rangle_A \otimes |10\rangle_{bc}),\end{aligned} \tag{13}$$

where we used the qubits b and c to encode the states of the qutrit B. The probabilities, given that the qubit is prepared in the $|0\rangle_A$, are

$$\Pr(M_1|0) = \langle 0|M_1^\dagger M_1|0\rangle = 2/3, \tag{14}$$

$$\Pr(M_2|0) = \langle 0|M_2^\dagger M_2|0\rangle = 1/6. \tag{15}$$

$$\Pr(M_3|0) = \langle 0|M_3^\dagger M_3|0\rangle = 1/6. \tag{16}$$

After state preparation, a projective measurement is performed on the basis $\{|00\rangle_{bc}, |01\rangle_{bc}, |10\rangle_{bc}, |11\rangle_{bc}\}$ of the auxiliary system. The obtained probabilities are shown in Fig. 4.

As a third example, let us consider a one-qutrit three-element POVM given by

$$M_1 = \tfrac{1}{2}(|0\rangle + |2\rangle)(\langle 0| + \langle 2|), \tag{17}$$

$$M_2 = \tfrac{1}{2}(|0\rangle - |2\rangle)(\langle 0| - \langle 2|), \tag{18}$$

$$M_3 = |1\rangle\langle 1|. \tag{19}$$

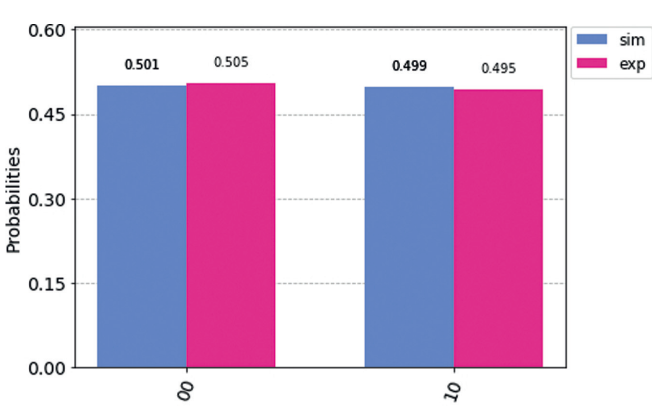

FIG. 3. Simulation (sim) and demonstration (exp) statistics for the one-qubit two-element POVM of Eq. (6) implemented using our protocol for the qubit prepared in the state $|0\rangle_A$.

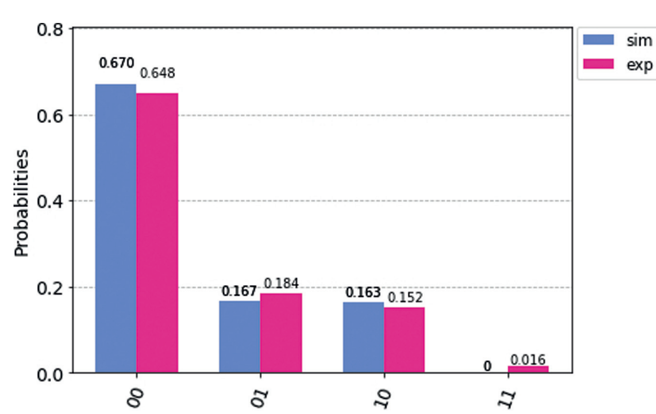

FIG. 4. Simulation (sim) and demonstration (exp) statistics for the one-qubit three-element POVM of Eq. (12) implemented using our protocol for the qubit prepared in the state $|0\rangle_A$.

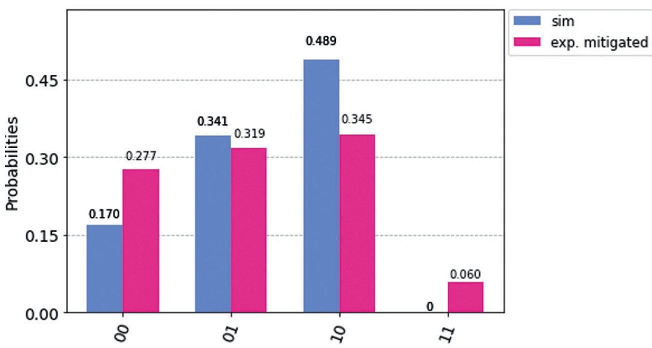

FIG. 5. Simulation (sim) and demonstration (exp. mitigated) statistics with mitigated errors from *ibmq_belem* quantum system [29] for the one-qutrit three-element POVM of Eq. (17) implemented using our protocol for the qutrit prepared in the state $|\psi_0\rangle_A$.

We set the premeasurement state of system A to $|\psi_0\rangle_A = \frac{1}{\sqrt{3}}(|0\rangle + e^{2i\pi/3}|1\rangle + e^{4i\pi/3}|2\rangle)$. In this case the global state to be prepared is

$$|\Psi\rangle_{AB} = \alpha(|0\rangle + |2\rangle)_A \otimes |0\rangle_B + \beta(|0\rangle - |2\rangle)_A \otimes |1\rangle_B - \gamma|1\rangle_A \otimes |2\rangle_B, \tag{20}$$

with $\alpha = \frac{\sqrt{3}-3i}{12}$, $\beta = \frac{\sqrt{3}+i}{4}$, and $\gamma = \frac{\sqrt{3}-3i}{6}$. Using qubits a and b to encode the states of target qutrit A and qubits c and d to encode the states of qutrit B, the state vector above can be represented by

$$|\Psi\rangle_{abcd} = \alpha(|00\rangle + |10\rangle)_{ab} \otimes |00\rangle_{cd} - \gamma|01\rangle_{ab} \otimes |10\rangle_{cd} + \beta(|00\rangle - |10\rangle)_{ab} \otimes |01\rangle_{cd}. \tag{21}$$

In this case, given the premeasurement state $|\psi_0\rangle_A$ above, the probabilities are

$$Pr(M_1|\psi_0) = \langle\psi_0|M_1^\dagger M_1|\psi_0\rangle = 1/6, \tag{22}$$

$$Pr(M_2|\psi_0) = \langle\psi_0|M_2^\dagger M_2|\psi_0\rangle = 1/2, \tag{23}$$

$$Pr(M_3|\psi_0) = \langle\psi_0|M_3^\dagger M_3|\psi_0\rangle = 1/3. \tag{24}$$

As in the previous example, after state preparation, a projective measurement is performed on the basis $\{|00\rangle_{cd}, |01\rangle_{cd}, |10\rangle_{cd}, |11\rangle_{cd}\}$ of the auxiliary system, and the obtained probabilities are shown in Fig. 5.

As a last example, let us consider a two-qubit four element POVM, with measurement operators given as follows:

$$M_1 = \sqrt{\frac{2}{3}}|\Phi_+\rangle\langle\Phi_+|, \tag{25}$$

$$M_2 = \sqrt{\frac{2}{3}}|\Psi(2\pi/3)\rangle\langle\Psi(2\pi/3)|, \tag{26}$$

$$M_3 = \sqrt{\frac{2}{3}}|\Psi(4\pi/3)\rangle\langle\Psi(4\pi/3)|, \tag{27}$$

$$M_4 = |\Phi_-\rangle\langle\Phi_-| + |\Psi_-\rangle\langle\Psi_-|, \tag{28}$$

with $|\Psi(\theta)\rangle = \cos(\frac{\theta}{2})|\Phi_+\rangle + \sin(\frac{\theta}{2})|\Psi_+\rangle$. The premeasurement state of the system AB is given by $|\psi_0\rangle_{AB} = |00\rangle$, so the global state to be prepared is

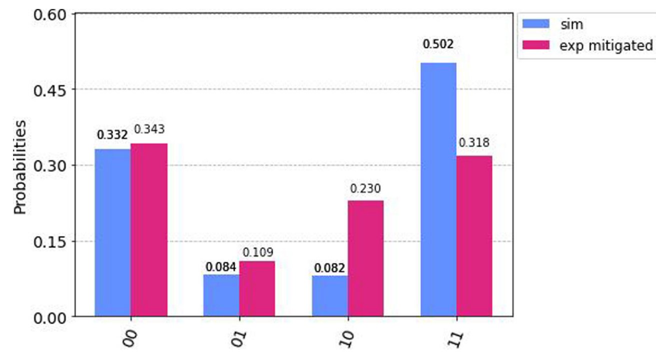

FIG. 6. Simulation (sim) and demonstration (exp mitigated) statistics with mitigated errors from *ibmq_belem* quantum system [29] for the two-qubit four-element POVM of Eq. (25) implemented using our protocol for the two qubits prepared in the state $|00\rangle_{AB}$.

$$\begin{aligned}|\Phi_{abcd}\rangle = &\sqrt{\frac{1}{6}}(|00\rangle_{ab} \otimes |00\rangle_{cd} + |11\rangle_{ab} \otimes |00\rangle_{cd}) \\ &+ \frac{1}{4\sqrt{6}}(|00\rangle_{ab} \otimes |01\rangle_{cd} + |11\rangle_{ab} \otimes |01\rangle_{cd}) \\ &+ \frac{1}{4\sqrt{2}}(|01\rangle_{ab} \otimes |01\rangle_{cd} + |10\rangle_{ab} \otimes |01\rangle_{cd}) \\ &+ \frac{1}{4\sqrt{6}}(|00\rangle_{ab} \otimes |10\rangle_{cd} + |11\rangle_{ab} \otimes |10\rangle_{cd}) \\ &- \frac{1}{4\sqrt{2}}(|01\rangle_{ab} \otimes |10\rangle_{cd} + |10\rangle_{ab} \otimes |10\rangle_{cd}) \\ &+ \frac{1}{2}(|00\rangle_{ab} \otimes |11\rangle_{cd} - |11\rangle_{ab} \otimes |11\rangle_{cd}),\end{aligned} \tag{29}$$

where we use the qubits b and c to encode the states of the auxiliary ququart system. For the premeasurement state $|\psi_0\rangle_{AB}$ above, we have the following probabilities:

$$Pr(M_1|00\rangle) = \langle 00|M_1^\dagger M_1|00\rangle = 1/3, \tag{30}$$

$$Pr(M_2|00\rangle) = \langle 00|M_2^\dagger M_2|00\rangle = 1/12, \tag{31}$$

$$Pr(M_3|00\rangle) = \langle 00|M_3^\dagger M_3|00\rangle = 1/12, \tag{32}$$

$$Pr(M_4|00\rangle) = \langle 00|M_4^\dagger M_4|00\rangle = 1/2. \tag{33}$$

As in the previous examples, after state preparation a projective measurement is performed on the computational basis of the auxiliary system $\{|00\rangle_{cd}, |01\rangle_{cd}, |10\rangle_{cd}, |11\rangle_{cd}\}$, allowing the extraction of the probabilities presented in Fig. 6.

Now, let us show how our protocol can be used for implementing *quantum instruments* (QI), that are quantum operations having as input a quantum state and as output a quantum state and a classical variable [2]:

$$\Gamma(|\psi_0\rangle_A) = \sum_j \varepsilon_j(|\psi_0\rangle_A) \otimes |j\rangle_J\langle j|, \tag{34}$$

in which $\{|j\rangle_J\}$ is an orthonormal basis for the system J and

$$\varepsilon_j(|\psi_0\rangle_A) = \sum_k M_{j,k}|\psi_0\rangle_A\langle\psi_0|M_{j,k}^\dagger \tag{35}$$

is a trace nonincreasing quantum operation, i.e., $\mathrm{Tr}[\varepsilon_j(|\psi_0\rangle_A)] \leqslant 1$. Above, $M_{j,k}$ are the elements of a POVM, i.e., $\sum_{j,k} M_{j,k}^{\dagger} M_{j,k} = \mathbb{I}$. One can verify that the quantum instrument in Eq. (34) can be obtained from the purification

$$|\Psi_{AJE_jE_J}\rangle = \sum_{j,k} M_{j,k}|\psi_0\rangle_A \otimes |j\rangle_J \otimes |k\rangle_{E_j} \otimes |j\rangle_{E_J}. \quad (36)$$

That is to say, $\Gamma(|\psi_0\rangle_A) = \mathrm{Tr}_{E_jE_J}(|\Psi\rangle_{AJE_jE_k}\langle\Psi|)$. So, given the QI, that is to say, given the completely positive maps ε_j in terms of the set of measurement operators $\{M_{j,k}\}_k$, we can simulate this QI by preparing the state $|\Psi_{AJE_jE_J}\rangle$ and by taking the partial trace over the auxiliary systems E_j, E_J. By measuring the system J in the basis $\{|j\rangle_J\}_j$ and postselecting the results, we can also reconstruct the action of the operators $\varepsilon_j(|\psi_0\rangle_A)$. In what follows, we exemplify the application of this simulation protocol. Let us consider a one-qubit QI defined by the following set of trace nonincreasing quantum operations:

$$\varepsilon_0 \equiv \left\{M_{00} = \frac{1}{\sqrt{2}}|0\rangle\langle 0|, M_{01} = \frac{1}{\sqrt{2}}|+\rangle\langle +|\right\}, \quad (37)$$

$$\varepsilon_1 \equiv \left\{M_{10} = \frac{1}{\sqrt{2}}|1\rangle\langle 1|, M_{11} = \frac{1}{\sqrt{2}}|-\rangle\langle -|\right\}. \quad (38)$$

We set the premeasurement state of system A to $|\psi_0\rangle_A = |0\rangle_A$. The global state to be prepared for the simulation of this QI is

$$\begin{aligned}\sqrt{2}|\Psi\rangle_{AJE_jE_J} &= |0000\rangle_{AJE_jE_J} + \frac{1}{2}|0010\rangle_{AJE_jE_J} \\ &\quad + \frac{1}{2}|1010\rangle_{AJE_jE_J} + \frac{1}{2}|0111\rangle_{AJE_jE_J} \\ &\quad - \frac{1}{2}|1111\rangle_{AJE_jE_J}. \end{aligned} \quad (39)$$

From this quantum state, we obtain the quantum instrument

$$\begin{aligned} 8\Gamma(|0\rangle_A) &= 8\mathrm{Tr}_{E_jE_J}\{|\Psi\rangle_{AJE_jE_J}\langle\Psi|\} \\ &= (5|0\rangle_A\langle 0| + |0\rangle_A\langle 1| + |1\rangle_A\langle 0| + |1\rangle_A\langle 1|)|0\rangle_J\langle 0| \\ &\quad + (|1\rangle_A\langle 1| - |0\rangle_A\langle 1| - |1\rangle_A\langle 0| + |0\rangle_A\langle 0|)|1\rangle_J\langle 1| \\ &= \varepsilon_0(|0\rangle_A) \otimes |0\rangle_B\langle 0| + \varepsilon_1(|0\rangle_A) \otimes |1\rangle_B\langle 1|. \end{aligned} \quad (40)$$

This state was reconstructed using quantum state tomography. The theoretical and demonstration results are shown in Fig. 7. For this demonstration we use the IBM quantum chip *ibmq_belem* [29]. In this case, the obtained demonstration result also agreed quite well with the theoretical prediction.

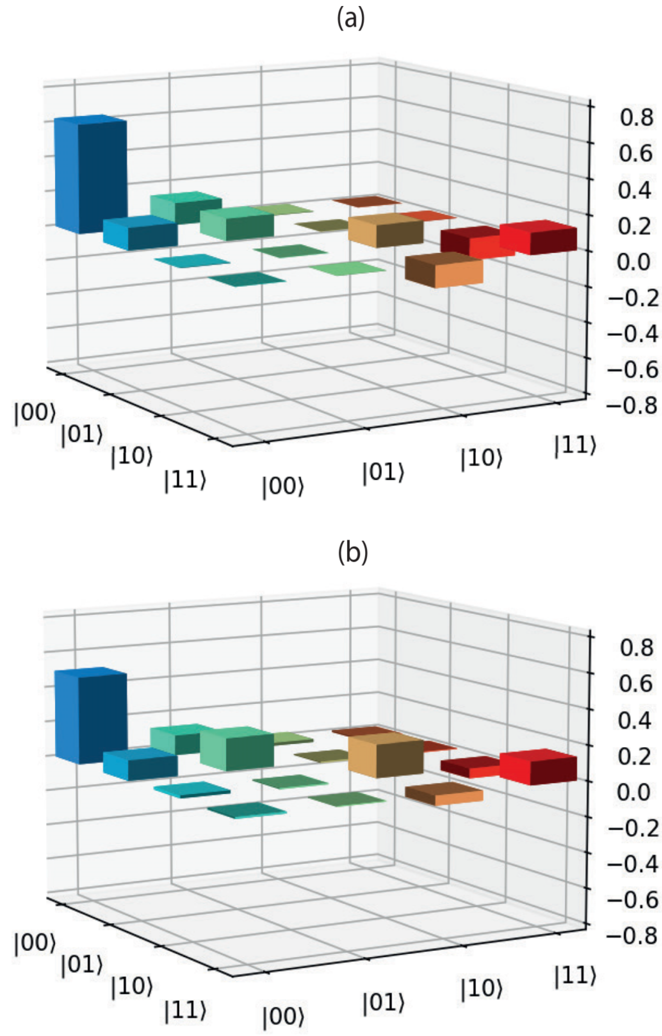

FIG. 7. (a) Theoretical and (b) demonstration results for the state tomography of the state (quantum instrument) in Eq. (40) simulated using the protocol we introduced in this article.

III. FINAL REMARKS

In summary, we pointed out that changes in the algorithm are needed for maintaining the claimed scaling of the number of auxiliary qubits and we highlighted the practical difficulties of the protocol presented in Ref. [20]. We circumvented these difficulties through the use of quantum state preparation algorithms. This approach avoids the numerical and computational issues associated with the solution of systems of nonlinear equations and easily generalizes the implementation of Ref. [20] for two-level states (one qubit) to d-level states, avoiding also the complications of their algorithm regarding the implementation of general unitary transformations on a multiqubit system. We exemplified the application of our protocol for one qubit, one qutrit, and two qubit POVMs and for simulating quantum instruments. These examples were demonstrated using IBM quantum computers. The simulation results matched the theoretical predictions. The demonstration results are in fairly good agreement with theory, but can be further improved if this protocol is executed in lesser noise quantum devices. So we believe that the simplicity and easy of use of this protocol will foster further research involving POVMs.

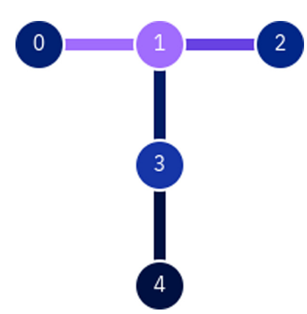

FIG. 8. Illustration of the connectivity between qubits of the *ibmq_belem* quantum chip.

TABLE I. Calibration parameters for the *ibmq_belem* quantum chip when used for the examples in Figs. 3–6.

	$Q0$	$Q1$	$Q2$	$Q3$	$Q4$
Frequency (GHz)	5.09	5.246	5.361	5.17	5.259
$T1$ (μs)	155.98	119.12	91.07	63.29	88.85
$T2$ (μs)	121.74	117.28	58.25	146.89	151.6
One-qubit error (10^{-4})	1.69	17.87	2.57	6.36	13.64
Readout error (10^{-2})	1.45	2.90	2.65	3.78	3.26
CNOT error (10^{-2})	0–1	1–3	2–1	3–4	4–3
	1.858	1.293	1.089	2.143	2.143
		1–2		3–1	
		1.089		1.293	
		1–0			
		1.858			

ACKNOWLEDGMENTS

This work was supported by the São Paulo Research Foundation (FAPESP), Grant No. 2022/09496-8, by the National Institute for the Science and Technology of Quantum Information (INCT-IQ), Grant No. 465469/2014-0, by the Coordination for the Improvement of Higher Education Personnel (CAPES), Grant No. 88882.427913/2019-01, by the National Council for Scientific and Technological Development (CNPq), Grant No. 309862/2021-3, and by the Brazilian Space Agency (AEB), Grant No. 01350.001732/2020-61 (TED 020/2020).

APPENDIX: INFORMATION ABOUT THE USED QUANTUM CHIP

In this article, we implement our POVM simulation algorithm using IBMQ platform [29]. We use quantum chips through QISKIT, an Open Source Quantum Development Kit for working with quantum computers at the level of pulses, circuits, and application modules. In our demonstrations, we used the *ibmq_belem* quantum chip with the same calibration parameters presented in Table I for the examples in Figs. 3–6. On the other hand, for the example in Fig. 7, we used the same chip but with calibration parameters as shown in Table II. The *ibmq_belem* quantum chip connectivity is shown in Fig. 8.

TABLE II. Calibration parameters for the *ibmq_belem* quantum chip when used for the example in Fig. 7.

	$Q0$	$Q1$	$Q2$	$Q3$	$Q4$
Frequency (GHz)	5.09	5.246	5.361	5.17	5.23
$T1$ (μs)	128.46	88.52	85.16	79.29	1.55
$T2$ (μs)	127.51	99.97	65.4	134.08	92.04
One-qubit error (10^{-4})	1.651	2.937	2.912	4.044	1.849×10^3
Readout error (10^{-2})	1.31	1.99	2.19	2.87	14.67
CNOT error (10^{-2})	0–1	1–3	2–1	3–4	4–3
	1.345	1.682	0.698	100.0	100.0
		1–2		3–1	
		0.698		1.682	
		1–0			
		1.345			

[1] M. A. Nielsen and I. L. Chuang, *Quantum Computation and Quantum Information* (Cambridge University Press, Cambridge, England, 2000).

[2] M. Wilde, *Quantum Information Theory* (Cambridge University Press, New York, 2013).

[3] R. Derka, V. Bužek, and A. K. Ekert, Universal Algorithm for Optimal Estimation of Quantum States from Finite Ensembles via Realizable Generalized Measurement, Phys. Rev. Lett. **80**, 1571 (1998).

[4] H. C. Nguyen, J. L. Bönsel, J. Steinberg, and O. Gühne, Optimising Shadow Tomography with Generalised Measurements, Phys. Rev. Lett. **129**, 220502 (2022).

[5] J. A. Bergou, Discrimination of quantum states, J. Mod. Opt. **57**, 160 (2010).

[6] A. Acín, S. Pironio, T. Vértesi, and P. Wittek, Optimal randomness certification from one entangled bit, Phys. Rev. A **93**, 040102(R) (2016).

[7] R. Jozsa, M. Koashi, N. Linden, S. Popescu, S. Presnell, D. Shepherd, and A. Winter, Entanglement cost of generalised measurements, Quantum Inf. Comput. **3**, 405 (2003).

[8] J. M. Renes, Spherical-code key-distribution protocols for qubits, Phys. Rev. A **70**, 052314 (2004).

[9] T. Vértesi and E. Bene, Two-qubit Bell inequality for which positive operator-valued measurements are relevant, Phys. Rev. A **82**, 062115 (2010).

[10] E. S. Gómez, S. Gómez, P. González, G. Cañas, J. F. Barra, A. Delgado, G. B. Xavier, A. Cabello, M. Kleinmann, T. Vértesi, and G. Lima, Device-Independent Certification of a Nonprojective Qubit Measurement, Phys. Rev. Lett. **117**, 260401 (2016).

[11] S. E. Ahnert and M. C. Payne, General implementation of all possible positive-operator-value measurements of single photon polarization states, Phys. Rev. A **71**, 012330 (2005).

[12] M. Ziman and V. Bužek, Realization of positive-operator-valued measures using measurement-assisted programmable quantum processors, Phys. Rev. A **72**, 022343 (2005).

[13] Y. Liu and J.-X. Cui, Realization of Kraus operators and POVM measurements using a duality quantum computer, Chin. Sci. Bull. **59**, 2298 (2014).

[14] Z. Bian, J. Li, H. Qin, X. Zhan, R. Zhang, B.C. Sanders, and P. Xue, Realization of Single-Qubit Positive-Operator-Valued Measurement via a One-Dimensional Photonic Quantum Walk, Phys. Rev. Lett. **114**, 203602 (2015).

[15] Y. Zhao, N. Yu, P. Kurzyński, G. Xiang, C.-F. Li, and G.-C. Guo, Experimental realization of generalized qubit measurements based on quantum walks, Phys. Rev. A **91**, 042101 (2015).

[16] M. Oszmaniec, L. Guerini, P. Wittek, and A. Acín, Simulating Positive-Operator-Valued Measures with Projective Measurements, Phys. Rev. Lett. **119**, 190501 (2017).

[17] Z. Li, H. Zhang, and H. Zhu, Implementation of generalized measurements on a qudit via quantum walks, Phys. Rev. A **99**, 062342 (2019).

[18] M. Oszmaniec, F. B. Maciejewski, and Z. Puchała, Simulating all quantum measurements using only projective

measurements and postselection, Phys. Rev. A **100**, 012351 (2019).

[19] Z. Hou, J.-F. Tang, J. Shang, H. Zhu, J. Li, Y. Yuan, K.-D. Wu, G.-Y. Xiang, C.-F. Li, and G.-C. Guo, Deterministic realization of collective measurements via photonic quantum walks, Nat. Commun. **9**, 1414 (2018).

[20] Y. S. Yordanov and C. H. W. Barnes, Implementation of a general single-qubit positive operator-valued measure on a circuit-based quantum computer, Phys. Rev. A **100**, 062317 (2019).

[21] A. Y. Kitaev, Quantum measurements and the abelian stabilizer problem, arXiv:quant-ph/9511026.

[22] V. V. Shende, S. S. Bullock, and I. L. Markov, Synthesis of quantum logic circuits, IEEE Trans. Comput.-Aided Des. Integr. Circuits Syst. **25**, 1000 (2006).

[23] M. Plesch and Č. Brukner, Quantum-state preparation with universal gate decompositions, Phys. Rev. A **83**, 032302 (2011).

[24] J. M. Arrazola, T. R. Bromley, J. Izaac, C. R. Myers, K. Brádler, and N. Killoran, Machine learning method for state preparation and gate synthesis on photonic quantum computers, Quantum Sci. Technol. **4**, 024004 (2019).

[25] I. F. Araujo, D. K. Park, F. Petruccione, and A. J. da Silva, A divide-and-conquer algorithm for quantum state preparation, Sci. Rep. **11**, 6329 (2021).

[26] R.-H. He, H.-D. Liu, S.-B. Wang, J. Wu, S.-S. Nie, and Z.-M. Wang, Universal quantum state preparation via revised greedy algorithm, Quantum Sci. Technol. **6**, 045021 (2021).

[27] X.-M. Zhang, M.-H. Yung, and X. Yuan, Low-depth quantum state preparation, Phys. Rev. Res. **3**, 043200 (2021).

[28] T. M. L. de Veras, L. D. da Silva, and A. J. da Silva, Double sparse quantum state preparation, Quantum Inf. Process. **21**, 204 (2022).

[29] IBM Quantum, https://quantum-computing.ibm.com/.

[30] D. C. McKay, T. Alexander, L. Bello, M. J. Biercuk, L. Bishop, J. Chen, J. M. Chow, A. D. Córcoles, D. Egger, S. Filipp, J. Gomez, M. Hush, A. Javadi-Abhari, D. Moreda, P. Nation, B. Paulovicks, E. Winston, C. J. Wood, J. Wootton, J. M. Gambetta, QISKIT Backend specifications for openqasm and openpulse experiments, arXiv:1809.03452 [quant-ph].